

Chain organization and thermodynamics in micelles and bilayers.

II. Model calculations

I. Szleifer and A. Ben-Shaul

Department of Physical Chemistry and The Fritz Haber Molecular Dynamics Research Center, The Hebrew University of Jerusalem, Jerusalem 91904, Israel

W. M. Gelbart

Department of Chemistry, University of California, Los Angeles, California 90024

(Received 2 January 1985; accepted 16 April 1985)

Based on the theory presented in part I (preceding paper) we calculate molecular and thermodynamic properties of model chains packed in micellar aggregates of three typical geometries: spheres, cylinders, and planar bilayers. Each possible conformation of a model chain is equivalent to a sequence of walks on a regular cubic lattice. The internal energy of a given conformation is proportional to the number of "kinks" ($\pi/2$ bond angles). The kink (*gauche*) energy measures the inherent flexibility of the chain. We calculate bond order parameter profiles for chains packed in aggregates of various curvature and radius, and find that in all cases the degree of conformational freedom increases from the chain head towards its end. The same qualitative behavior is observed for entirely flexible (zero kink energy) chains. This implies that the internal energy of the chain plays only a secondary role, compared to that of the packing constraints in determining chain conformational statistics in micellar aggregates. In accordance with this conclusion we also find that the geometry dependence of the conformational free energy is dominated by the entropic contribution. The differences between the minimal free energies of chains in different geometries are generally small. Yet, they may be comparable in magnitude to the changes associated with the surface ("opposing forces") contributions to the geometry dependence of the micelle's free energy.

I. INTRODUCTION

In the preceding paper¹ (part I) we presented a statistical-thermodynamic theory for chain organization in amphiphilic aggregates of various geometries. In this paper we apply the theory to model chains in order to analyze, in a systematic fashion, the parameters governing chain conformational statistics in micelles and bilayers. We have calculated various molecular properties such as bond order parameter profiles, spatial distributions of chain segments, and average chain dimensions. Thermodynamic characteristics of chain organization, e.g., conformational energies, entropies, and free energies have also been calculated. Our analysis is mainly intended to examine the roles of micellar geometry (i.e., radius and curvature), internal chain energies (flexibility), and packing constraints, in determining the structure and stability of the hydrophobic core.

All the calculations presented below are for approximate model chains which allow a (relatively) simple and consistent examination of the geometrical and molecular parameters. As has been shown in part I, when applied to more realistic model chains, our theory yields results which are in very good agreement with experimental and molecular dynamics data. The results of the calculations presented below for the approximate chains also show good qualitative agreement with experiment. Yet, no specific comparisons or attempts to show good fits with experimental data will be presented because our chief goal here is the theoretical analysis.

For the sake of completeness we quote here a few basic results and definitions from paper I. The probability distribution function (pdf) of chain conformations is given by

$$P(a) = \frac{1}{y'} \exp \left[-\beta \epsilon(a) - \beta \sum_{i=1}^{L-1} \pi'_i \phi_i(a) \right]. \quad (1)$$

Here $\beta = 1/kT$, and $\epsilon(a)$ is the internal energy of a chain in conformation a . $\phi_i(a)$ is the volume occupied by the chain in layer i of the hydrophobic core (Fig. 1). π'_i is the relative lateral pressure in layer i (with respect to π_L). The π'_i 's are determined by solving the equations expressing the packing constraints $\langle \phi_i \rangle = m_i$, m_i being the average volume available per chain in layer i . y' is the normalization constant (partition function). The quantity

$$\begin{aligned} -kT \ln \bar{z} &= \sum_a P(a) \epsilon(a) + kT \sum_a P(a) \ln P(a) \\ &= \langle \epsilon \rangle - T\bar{s} \end{aligned} \quad (2)$$

is the conformational (Helmholtz) free energy per chain (in the "mean-field" approximation); $\bar{z} = y' \exp(\beta \sum \pi'_i m_i)$.

II. THE CHAIN MODEL

The expression quoted in the previous section for $P(a)$ is general and applies to any chain model. In most, though not in all, cases of interest the hydrophobic tails of the amphiphiles are normal alkyl chains containing typically 10–20 CH_2 groups. In this section we describe the approximate model used here to represent such chains; the results of the calculations are reported in the next section. The present chain model is similar to the one used in our former study² but with two significant modifications: (i) conformational (*gauche/trans*) chain energies, $\epsilon(a)$, are included; (ii) the same type of chain conformations (i.e., bond angles) are used for

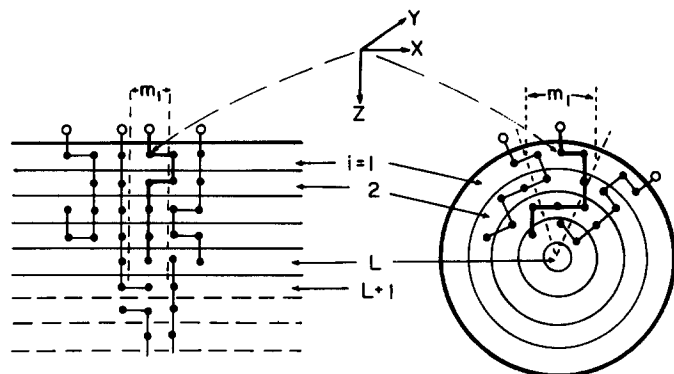


FIG. 1. A schematic, two dimensional, representation of the model used to describe chain organization and conformations in bilayers (left) and spherical or cylindrical micelles (right). (The model and the calculations refer to three dimensions.) The figure illustrates the geometric boundary conditions and packing constraints by showing a central chain (heavy line) in a "bath" of neighboring chains. All chain conformations are allowed provided no segment protrudes beyond the core's surface. The statistical weight of a given conformation depends on its internal energy, $\epsilon(a)$, and the volumes, $\phi_i(a)$'s, it occupies in the (imaginary) layers i . The bond angles of the model chains are either 0 or $\pi/2$ (kink), as if they were placed on a regular cubic lattice. (Unlike in Refs. 2, 3, and 4, this holds for all geometries). In all conformations included in the calculation of $P(a)$, the zeroth bond—connecting the head group (open circle) with the first chain segment—is normal to the core's surface. The origin of the coordinate system is attached to the first chain segment with the Z axis pointing towards the bilayers' midplane or the micelle's center. In cylinders Y is parallel to the cylinder axis. The bond length is always taken equal to the layers' width, $d = 1$. Note that in spheres and cylinders the radius of the innermost layer is $1/2$.

all micellar geometries. An important approximation which we keep using is that every segment of the model chain represents several (methylene) segments of the real chain. This approximation is retained partly for the sake of comparison with our previous calculations and partly because it reduces significantly the computational effort.

In our previous study we have used the chain model proposed by Dill and Flory,^{3,4} who employed a different approach and consequently derived different expressions for $P(a)$. Following these authors the hydrophobic cores were represented² by (cubic) lattices and the assumption of uniform, liquid-like, density was implemented by a "space-filling" requirement, i.e., that all lattice sites will be occupied by chain segments. The average volume per CH_2 group of an alkyl chain in the liquid state⁵ is $\approx 27 \text{ \AA}^3$, and its effective length in the (all-*trans*) chain is $\approx 1.27 \text{ \AA}$ [$= l \sin(\theta/2)$, where $l \approx 1.53 \text{ \AA}$ is the C-C bond length and $\theta \approx 112^\circ$ is the C-C-C bond angle]. Thus, the cross sectional area of a CH_2 group is 21.2 \AA^2 , corresponding to a square each side of which is $\approx 4.6 \text{ \AA}$ long.² A cube with these dimensions was used as the unit cell of the cubic lattice. Hence each segment of the model chain represents $4.6/1.27 \approx 3.6$ CH_2 groups of an alkyl chain. This implies that the bond length and segmental volume of the model chain are 4.6 \AA and $\nu = 4.6^3 = 97 \text{ \AA}^3$, respectively.

The regular cubic lattice describing the hydrophobic core of a planar bilayer has been appropriately "curved" in order to represent spherical and cylindrical micelles.^{3,4} Consequently the fixed (0 and $\pi/2$) bond angles of the chains placed on the regular cubic lattice are replaced by arbitrary (almost random) bond angles on the curved lattices. As long as all chain conformations are assumed equi-energetic

[$\epsilon(a) = \text{const}$], this is not a serious limitation. However, when this assumption is removed, as in the present study, the arbitrary bond angles prevent an unambiguous assignment of bond energies. This difficulty is easily resolved by using the same, regular cubic, model chain for all micellar geometries, and introducing the effects of the curved surface only through the boundary conditions on allowed chain conformations. Formally, this corresponds to "cutting" a regular cubic lattice into a sphere, cylinder, etc. It should be emphasized however that the lattice is just a pictorial means for describing the organization of the chains within the core, but in practice it is not needed at all. Nowhere in our derivation of $P(a)$ have we used the notion of a lattice.¹ Moreover, neither the packing constraints [$\langle \phi_i \rangle = m_i$] nor $\epsilon(a)$ require the use of a lattice.

In all our calculations the layer width d was set equal to the bond length, i.e., $d = \nu^{1/3}$. Henceforth, $d (= \nu^{1/3})$ and ν will be used as our unit length and unit volume, respectively. The various chain conformations are conveniently generated and described using a Cartesian coordinate system whose origin is attached to the first chain's segment, see Fig. 1. In all calculations this segment is assumed to be fixed at some point in the center of layer 1. The Z axis is normal to the core's interface and points towards the center of the aggregate. In spherical and planar aggregates the X, Y axes are equivalent and can thus be chosen arbitrarily. In cylinders, where the symmetry is lower, we choose the Y axis parallel to the long cylinder axis.

A few representative chain conformations are shown schematically in Fig. 1. The "zeroth bond" connecting the head group with the first segment (located in layer 1) is assumed to be always perpendicular to the interface, i.e., parallel to the Z axis (so that the head group is located at $(X, Y, Z) = (0, 0, -1)$). The first chain bond has five possible directions (as in a regular cubic lattice), four of which are perpendicular to the zeroth bond (parallel to the $\pm X, \pm Y$ axes) and one parallel. Similarly, the second bond has four possible directions perpendicular to the first bond and one direction forming zero bond angle, and so on. In this way we generate all possible chain conformations, a . Conformations involving bond intersections ("avoided walks") or protrusion of any chain segment outside the core's interface are regarded as forbidden and thus excluded from the calculation. All other conformations are allowed, including those with reversals towards the surface or with two next-nearest neighbor bonds in parallel directions. (The latter case resembles the high energy "pentane configuration"⁶ in normal alkyl chains. Recalling, however, that each bond of the model chain corresponds to ~ 3.6 C-C bonds of an alkyl chain this analogy is irrelevant here.) Chain *interdigitation* across the midplane of bilayers is also taken into account (see below).

A fully extended chain (i.e., all bond angles are zero), corresponds to an alkyl chain in the all-*trans* conformation. This is the conformation of minimal energy which we take as $\epsilon = 0$. All other conformations involve at least one "kink" (a $\pi/2$ angle between adjacent bonds). The kinks deform the fully extended chain and are thus analogous to *gauche* bonds in polymethylene chains. In the spirit of the rotational isomeric state model,⁶ we assume that each kink is associated

with a fixed energy $\chi > 0$. (Actually χ is a free energy.) χ is assumed to be the same for all kinks along the chain, except for a kink between the zeroth bond and the first chain bond. This is because the head group is not equivalent to the other chain segments.⁷ A kink in this position will be assigned an energetic price χ_0 . Thus, the internal energy of a chain in conformation a is given by

$$\epsilon(a) = k_0(a)\chi_0 + k(a)\chi, \quad (3)$$

where $k_0(a) = 0$ or 1 if there is, or there is not, a kink between the zeroth and the first bonds. $k(a)$ is the number of internal kinks: $k(a) \leq n - 2$, where n is the number of chain segments (the number of chain bonds, not including the zeroth is $n - 1$).

A numerical value for χ was determined by requiring that a "random" model chain should have the same mean end-to-end distance ($\langle r^2 \rangle$) as the corresponding random alkyl chain. By a "random chain" we mean a chain which is not subject to any spatial constraints (such as those present in micelles due to anchoring the chain origin at the surface, or to the presence of neighboring chains). Also, the random chain refers only to the hydrophobic tail of the amphiphile, i.e., it lacks the polar head and the zeroth bond, hence its energy does not involve the first term in Eq. (3). The idea of determining χ by equating the end-to-end distances of the real and model chains was adopted from Ref. 8 (where it was applied to chains on two diamond lattices with different bond lengths). The mean end-to-end distance is the most common characteristic of chain conformational statistics and thus serves as the most "natural" criterion. It should be noted however that this is not the only possible criterion. For instance, we could require that the average chain energy, entropy, or radius of gyration would be the same. (These criteria yield somewhat different values for χ .)

The calculations presented in the next section are for model chains with $n - 1 = 6$ bonds, corresponding to alkyl chains with $\sim 3.6 \times 6 \sim 22$ bonds. Calculating $\langle r^2 \rangle$ for our model chain as a function of χ and comparing with detailed calculations⁹ of this quantity for alkyl chains we obtain $\chi \cong 0.30 kT$ (for $T = 300$ K). A very similar value was also obtained for $n - 1 = 4$. (Independence of χ on n is expected for large n but is not obvious for the small n 's considered here.) The zeroth bond is not equivalent to the others. Thus, χ_0 was treated as a parameter in the calculations. This parameter has small effect on the results, reflected mainly (as expected) in the properties of the first bond. Most of the numerical results are presented for chains with $\chi_0 = 0.7$, a value chosen according to a criterion described in the next section.

Substituting Eq. (3) into Eq. (2) we can rewrite $P(a)$ in the form

$$P(a) = \frac{1}{y'} \omega_0^{k_0(a)} \omega^{k(a)} \prod_{i=1}^{L-1} \alpha_i^{\phi_i(a)}, \quad (4)$$

where $\omega = \exp(-\beta\chi)$, $\omega_0 = \exp(-\beta\chi_0)$, and $\alpha_i = \exp(-\beta\pi_i)$. In our calculations the ϕ_i 's were treated as integers (i.e., integer multiples of ν). Namely, for a given conformation a , $\phi_i(a)$ is the number of chain segments whose centers fall in layer i .

The application of Eq. (4) to planar bilayers deserves a

special comment. According to our construction, the number of layers in such aggregates is $2L$ rather than L as implied by Eq. (4), see Fig. 1. Thus, in its present form this equation is inapplicable to (interdigitating) conformations in which a chain crosses the bilayer's midplane. In order to include these conformations we should extend the product of α_i 's to all layers $i = 1, \dots, 2L$. Clearly, however, the two monolayers composing a (symmetric) bilayer are equivalent: hence $\alpha_i = \alpha_{2L-i+1}$. Thus, defining

$$\bar{\phi}_i(a) = \phi_i(a) + \phi_{2L-i+1}(a), \quad (5)$$

Eq. (4) is also applicable to interdigitating conformations, provided ϕ_i is replaced by $\bar{\phi}_i$. A more detailed proof of the above statement has been given in Ref. 1. In our calculations the bilayer is always divided into an even number, $2L$, of monolayers. Of course, one can easily extend Eq. (5) to odd numbers, $2L + 1$, of layers.

With the aid of $P(a)$ one can calculate any desired chain property. A property of particular interest is the profile of bond order parameters along the chain. Using k to denote the bond connecting segments k and $k + 1$ of the chain ($k = 1$ for the segment connected to the head) the k th bond's order parameter is defined as

$$\begin{aligned} S_k &= \langle P_2(\cos \theta_k) \rangle \\ &= (3/2) \sum_a P(a) \cos^2 \theta_k(a) - 1/2 \\ &= (3/2) P_k(\parallel) - 1/2, \end{aligned} \quad (6)$$

where θ_k is the angle between the k th bond and the normal to the interface $P_2(\cos \theta)$ is the second Legendre polynomial and $P_k(\parallel)$ is the overall probability of finding the k th bond parallel to the normal.

Given the pdf of chain conformations we can calculate $P_k(x,y,z)$, the probability of finding the k th chain segment at point x,y,z . We have calculated some moments of this distribution in order to examine the effects of chain packing and micellar geometry on chain properties. The first moments $\langle x_k \rangle$ and $\langle y_k \rangle$ vanish, as in isotropic media, but $\langle z_k \rangle \neq 0$, due to the anchoring of the first segment in layer 1, and the existence of the "reflecting wall" at the interface. ($z_1 = \langle z_1 \rangle = 0$ by construction). In particular $\langle z_n \rangle$, where n is the last chain segment, measures the extension of the chain towards the center of the core. Also, unlike in isotropic liquids, $\langle z_k^2 \rangle \neq \langle x_k^2 \rangle$, $\langle y_k^2 \rangle$. In cylinders we also have $\langle x_k^2 \rangle \neq \langle y_k^2 \rangle$. We shall be particularly interested in the mean square end-to-end distance

$$\langle r_n^2 \rangle = \langle x_n^2 \rangle + \langle y_n^2 \rangle + \langle z_n^2 \rangle \quad (7)$$

as a measure of the "liquid-like" behavior of the chains within the core. $\langle x_n^2 \rangle$, and more generally $\langle x_k^m \rangle$, etc. are given by

$$\langle x_k^m \rangle = \sum_a P(a) [x_k(a)]^m, \quad (8)$$

where $x_k(a)$ is the x component of the k th segment for chain conformation a .

A related quantity of interest is the "radial distribution" of chain segments, i.e., the probability of finding the k th segment at a distance r from the center of the core (the midplane in bilayer, the cylinder axis in cylindrical micelles).

Information on this quantity is obtained from neutron scattering experiments¹⁰ on micellar systems containing amphiphiles with selectively deuterated methylene groups. In our model the distance from the center of the core is given by $L - i$ ($L - i + \frac{1}{2}$ for bilayers, see below) where i is the layer's number and L is the radius of the core (half thickness in bilayers). Thus, the radial distribution is given by

$$P_k(i) = \sum_a P(a) h_k(a|i), \quad (9)$$

where $h_k(a|i) = 1$ if the k th segment falls in layer i and 0 otherwise. In particular, $P_n(i)$ gives the radial distribution of the terminal chain segment.

In addition to conformational properties we shall also calculate thermodynamic quantities such as $\langle \epsilon \rangle$, \bar{s} , and $-kT \ln \bar{z} = \langle \epsilon \rangle - T\bar{s}$. Our main interest is in the geometry dependence of all these properties. As argued in part I, the average area per head group A depends on the geometry, and vice versa. In our model¹¹ $A = M_1/Nd = m_1$ [recall that we have set $d = \nu^{1/3} = 1$ so that, for alkyl chains, $A = m_1$ —in units of $d^2 = (4.6)^2 \approx 21.2 \text{ \AA}^2$]. More generally, the average cross sectional area per chain in layer i is $A_i = m_i/d$ (except for the innermost layers in the spherical and cylindrical geometries whose radius is $d/2$ rather than d , so that $A_L = 2m_L d$, see Fig. 1). For chains packed at uniform, liquid-like, density throughout the hydrophobic core, $M = \sum M_i = Nn\nu$, hence $m_i = M_i/N = (M_i/M)n\nu$. For the M_i 's corresponding to the division into layers depicted in Fig. 1 we find (setting $\nu = 1$)

$$m_i = \begin{cases} n/L & \text{bilayer} \\ 2n(L-i)/(L-\frac{1}{2})^2 & \text{cylinder} \\ 3n[(L-i)^2 + \frac{1}{2}]/(L-\frac{1}{2})^3 & \text{sphere} \end{cases} \quad (10)$$

In the "continuum limit" ($L \gg 1$) we see that if all aggregate forms have the same radius L , then the average head-group areas ($A = m_i$) satisfy $A(L/n) = 1, 2$, and 3 for the planar bilayer, cylinder, and sphere, respectively.

III. RESULTS AND DISCUSSION

All the numerical results presented in this section are for model chains with $n = 7$ segments (not including the head group) or, equivalently, $n - 1 = 6$ bonds (not including the zeroth bond). As mentioned in the previous section these chains mimic alkyl chains comprising $\sim 6 \times 3.6 \sim 22$ C-C bonds. The pdf of chain conformations $P(a)$ was calculated using Eq. (1) with the α_i 's evaluated by solving the equations expressing the packing constraints, $\langle \phi_i \rangle = \sum P(a) \phi_i(a) = m_i$. For every geometry the radius (thickness) dependence was analyzed by varying L up to a maximal value of 7. ($L > 7$ implies "holes" in the hydrophobic core, at variance with the assumption of uniform and liquid-like density. See however, Ref. 12.) Most of the calculations are for the energy parameters $\omega = 0.3$ and $\omega_0 = 0.7$. Other values are used for comparison. Using $P(a)$ we have calculated several molecular and thermodynamic properties which reflect the effects of geometrical and packing constraints on the chain's conformation statistics.

Figure 2 shows profiles of bond order parameters for chains packed in planar bilayers of various widths [cf. Eq.

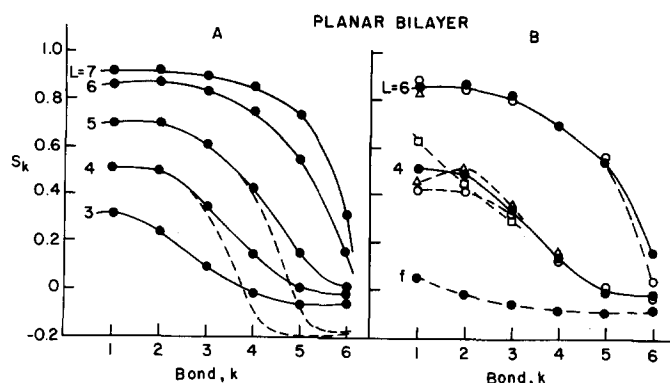


FIG. 2. Bond order parameter profiles for chains packed in bilayers. All calculations, here and below, are for chains with $n - 1 = 6$ bonds (not including the zeroth bond). (A) Order parameters for the "standard chain" with kink energy parameters $\omega_0 = 0.7$, $\omega = 0.3$ for different L (half-thickness) values. Note L is inversely proportional to the average head-group area, m_1 . In all cases except $L = 7$, $m_i = m_1 = n/L$ [cf. Eq. (11)] corresponding to uniform, liquid-like, density. For $L = 7$ Eq. (11) implies $m_i = 1$, i.e., a fully extended chain with $S_k \equiv 1$. The case shown in the figure is for $m_i = 1.1$ except $i = L$; $m_L = 0.4$, i.e., the L th layer is only partly filled. The dashed curves demonstrated for $L = 4, 5$ refer to chains artificially prevented from crossing the midplane (no interdigitation). (B) Effects of changing the energy parameters for two representative cases, $L = 4, 6$. (●)—the standard case, $\omega_0 = 0.7$, $\omega = 0.3$. (○)— $\omega_0 = \omega = 1.0$. (□)— $\omega_0 = \omega = 0.3$. (△)— $\omega_0 = 1.0$, $\omega = 0.3$. f—free chain ($L = 7$).

(6)]. For comparison we also show S_k for chains with $\omega, \omega_0 \neq 0.3, 0.7$, for free chains¹³ ($\alpha_i \equiv 1$) and for chains artificially confined to one monolayer ("no interdigitation"). The S_k 's calculated for the "standard parameters" $\omega = 0.3$, $\omega_0 = 0.7$ display the familiar behavior: They vary slowly with k at low k 's (bonds close to the head group) and at some intermediate k start declining to zero,¹⁴ reflecting the higher conformational freedom of segments near the chain terminus. Another type of order parameter measures the degree of chain ordering parallel to the "director" (i.e., the normal to the bilayer's surface), as a function of the distance from the surface.^{2,4-12,15} In bilayers, this ("radial" of "spatial") order parameter decreases towards the midplane. Namely, the probability of lateral chain placements (parallel to the surface) increases as the distance from the surface increases. These results are not shown here as they are very similar to previous findings.^{2,3,12} Another familiar and expected trend reflected in Fig. 2 is the decrease in the absolute values of S_k as L decreases. A decrease in L implies an increase in the average area per head-group $A \propto m_1 \propto 1/L$ [see Eq. (11)]. This, in turn, implies that more bonds must be placed laterally in order to fill the increased available volumes, thereby reducing their order parameter.

Forbidding chain interdigitation is equivalent to regarding the midplane as an impenetrable wall. The major effect of this restriction is to increase the probability of lateral placements for those bonds that can reach the midplane, i.e., the ones near the chain end. This is reflected by a decrease in the order parameters as depicted for two representative cases in Fig. 2(A). [The negative values for $k \sim n - 1$ imply $P_k(\parallel) < 1/3$, cf. Eq. (6).] Figure 2(B) demonstrates the sensitivity of S_k to the energy parameters ω and ω_0 . When the average area per head group is small (represented by $L = 6$, $m_1 = 7/6$) S_k is essentially independent of

ω and ω_0 . This is expected because when $m_1 (= m_i)$ is small only few conformations ("elongated ones") are probable and these must fill the available volume via kinks, regardless of the energetic price involved. As m_i is increased ($L = 4$, $m_1 = 7/4$) additional conformations become probable. However, packing constraints continue to dominate the energetic effects. (Compare, e.g., S_k for $\omega = \omega_0 = 1$ with the standard case.) The effect of varying ω_0 on S_k decreases rapidly with k , as could be anticipated. The qualitative behavior of S_k is unaffected. In our model, ω_0 may be interpreted, crudely, as measuring both the energetic factor associated with the angle between the zeroth and the first bond, and (implicitly) the angular distribution of the zeroth bond with respect to the director. There is no obvious general procedure for determining ω_0 . Our choice of $\omega_0 = 0.7$ was based on the requirement that for low k 's and intermediate L values, $S_k \simeq \text{const}$.

Figure 2(B) also shows S_k of a free chain¹ (for $L = 7$; the results for all $L > 2$ are essentially the same). If the chain were random, i.e., without the "impenetrable wall" representing the core's interface, we would get $S_k \equiv 0$. The finite, but small, S_k values show that the free chain is nearly, though not completely, random. (The numerical values of S_k for the first few bonds can easily be correlated with the boundary conditions and kink energies.)

Order parameter profiles for the curved geometries are shown in Fig. 3. The general behavior is in accord with available experimental data.^{3,19} Namely, S_k decreases with k , except possibly for the first few bonds. For a given core radius L the degree of ordering decreases with L . The sensitivity of S_k to ω and ω_0 increases with curvature: In these cases the degree of conformational freedom is higher than in bilayers because of the higher m_1 values (higher available volumes per chain, particularly near the interface). In the curved micelles S_k (mainly S_1) is quite sensitive to ω_0 . It should be noted that even if ω_0 were known exactly for bilayers its value for cylinders and spheres could be somewhat different, due to the different curvatures of the interfaces.

The higher values of S_k for a free chain in spheres and cylinders, as compared to those in bilayers, reflect the boundary conditions associated with restricting the chains to the concave side of the interface. The existence of such, bent, "walls" eliminates many chain conformations in which the first few bonds propagate in the XY plane (see Fig. 1). Consequently, these bonds are more strongly oriented along

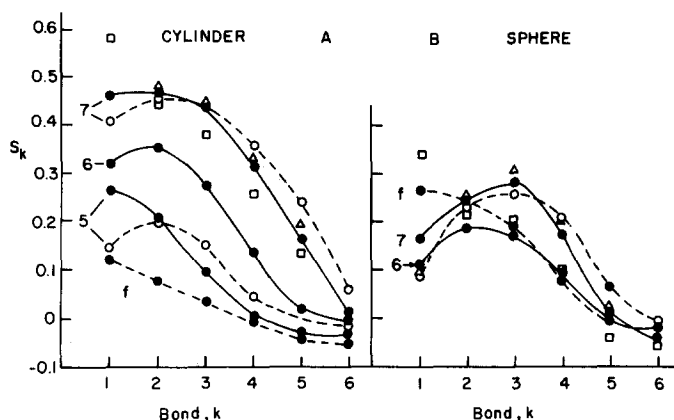


FIG. 3. Bond order parameter profiles for chains packed in cylindrical and spherical micelles. Notation and symbols as in Fig. 2. In all cases the chains are packed at uniform, liquid-like density, implying m_1 and L related via Eq. (11).

the Z axis, thereby increasing their order parameters.

Radial distribution of chain ends, $P_n(i)$, are shown in Figs. 4(A)–4(C). In bilayers, $P_n(i)$ always peaks rather sharply near the midplane, i.e., at $i = i_m = L$. Hence $\langle i \rangle = \langle z_n \rangle - 1 \simeq i_m = L$ [see Eqs. (7), (8), and Fig. 1]. It is not difficult to show that in the absence of chain reversals²⁻⁴ the liquid density assumption implies $\langle z_n \rangle = L - 1$. Otherwise $\langle z_n \rangle < L - 1$, see also Table I. The finite values of $P_n(i > L + 1)$ are due to interdigitation. The extent of interdigitation is appreciable and increases, as expected, as the area per head group increases (L decreases). The free chain is the least extended, since it is not subjected to lateral pressures (π_i) due to neighboring chains. The lateral pressures increase with L ($\propto 1/m_1$) and consequently also the deviations of $P_n(i)$ from the free chain behavior. When L is small, $L \sim 2, 3$, the real and free chains are quite similar. We thus expect that the minimum in the conformational free energy occurs around these L values. As we found for S_k , the sensitivity of $P_n(i)$ to variations in the energy parameters ω and ω_0 is small, especially for high L 's. As $\omega, \omega_0 \rightarrow 1$ (zero kink energies) the extent of interdigitation decreases slightly since lateral bond placements become, on the average, more probable.

In spherical micelles, Fig. 4C, $P_n(i)$ decreases with i . Also, for large L 's the behavior is quite similar to that of a free chain. (The small L 's are not important, see below.) In other words, in spherical micelles, the geometrical parameters (i.e., the concave interface and the rapidly decreasing

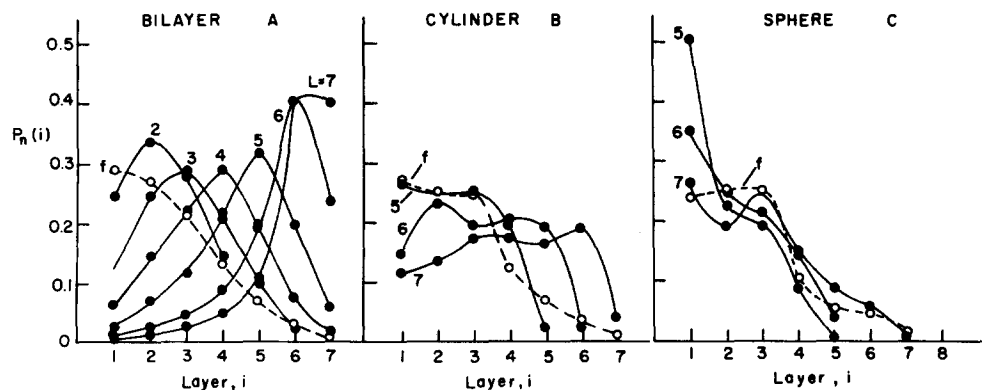


FIG. 4. Radial distributions of the terminal chain segment in bilayers, cylinders, and spheres. The numbers marking the curves indicate the core's radius (half-thickness). f denotes the free chain (for $L = 7$ in all geometries). The case $L = 7$ in bilayer corresponds to $m_1 = 1.10$ for $i < L - 1$ and $m_L = 0.4$.

m_i 's) are the major factors in determining chain properties. Packing constraints due to neighboring chains play a secondary role, because of the (relatively) large distances between head groups on the core's surface. The decrease of $P_n(i)$ with i results mainly from the decrease in the available volumes, m_i . We do not have a simple explanation for the minimum in $P_n(i)$ at $i = 2$ for $L = 7$. This may be due to the inherent limitations of our chain model and the restrictions on the zeroth bond (being normal to the interface and bisected thereby). A similar behavior was found for a more realistic chain model.^{15(c)} The curve may become "smoother" upon averaging over the position and orientation of the zeroth bond. The restrictions on this bond and the assumption that the core's interface is perfectly smooth and impenetrable may lead to artifacts at small L values (say $L < 4$). However, these small micelles are not very interesting for several reasons. The most relevant one is that such micelles are unstable because of the large area (m_1) exposed to water, and the high conformational free energy (see below).

The cylindrical geometry is intermediate between the spherical and planar geometries and so also is the corresponding $P_n(i)$. That is, in spheres $P_n(i)$ peaks at $i = 1$, in bilayers at $i = L$, and in cylinders it is a broad distribution spread mainly over intermediate layers, Fig. 4(B). Similar behavior was found in our previous study (where $\omega = \omega_0 = 1$). The free chain resembles a chain packed in a cylinder with $L = 5$, indicating that $m_1 \sim n/L \sim 1.4$ is the optimal head group area for this geometry. The (small) "irregularities" in $P_n(i)$ may again be due to the assumed limitations on the possible conformations of the model chain.

Neutron scattering experiments on spherocylindrical LDS micelles with small axial ratios (nearly spherical) suggest that the radial distribution of chain ends peaks approximately in the middle of the distance between the surface and the center of the core.¹⁰ A spherocylinder is a "superposition" of a sphere and a cylinder. Our results would therefore suggest a broad maximum located close to the core's surface. [It should be noted however that our model chains ($n = 7$) correspond to an alkyl chain of ~ 22 C atoms, i.e., about two times longer than the dodecyl chains studied in Ref. 10.] More detailed calculations as well as more accurate inversions of the scattering data are called for, before drawing quantitative conclusions from comparisons of experimental and theoretical data on segments' radial distributions.

The effects of geometrical packing constraints on chain dimensions are summarized in Table I. The table also lists the dimensions of the free chains in the various geometries (with radius $L = 7$). The values of L (equivalently m_1) for which the dimensions of the "real" chain are most similar to those of the corresponding free chain are geometry dependent. For bilayers, the conformational properties of the real and free chains are similar when $L \sim 2$ ($m_1 \sim 3.5$), for cylinders when $L \sim 4-5$ ($m_1 \sim 3$), and for spheres when $L \leq 7$ ($m_1 \sim 2.7$). Interestingly, in all these cases the mean end-to-end distance is about the same $\langle r^2 \rangle^{1/2} \sim 3.6-3.8$, which brackets the corresponding values of the free chains and of the random chain. (The random chain corresponds to a chain in the bulk liquid.) Yet, more detailed quantities such as $\langle x^2 \rangle$ and $\langle z \rangle$ are quite sensitive both to the shape and the

TABLE I. Chain dimensions in aggregates of different geometries. All data are for model chains with six bonds (not including the bond between the polar head and the first chain segment). In all cases $\omega = 0.3$ and $\omega_0 = 0.7$. m_1 is the area per head group in units of the cross sectional area of a fully extended chain (corresponding to $\sim 21 \text{ \AA}^2$).

L	Bilayer			Cylinder			Sphere				
	$\langle z \rangle$	$\langle x^2 \rangle^{1/2}$	$\langle r^2 \rangle^{1/2}$	m_1	$\langle z \rangle$	$\langle x^2 \rangle^{1/2}$	$\langle r^2 \rangle^{1/2}$	m_1	$\langle z \rangle$	$\langle x^2 \rangle^{1/2}$	$\langle r^2 \rangle^{1/2}$
7	5.03	5.16	5.29	1.10	3.02	3.45	4.12	1.99	2.30	2.69	3.58
6	4.59	4.79	4.98	1.17	2.45	2.86	3.80	2.32	2.03	2.38	3.32
5	3.55	3.81	4.31	1.40	1.99	2.40	3.60	2.77	1.89	2.18	3.26
4	2.70	3.04	3.89	1.75	1.58	2.07	3.69	3.43	1.47	1.86	2.82
3	2.00	2.38	3.67	2.33	1.34	2.18	3.94	4.48	1.97	2.33	3.00
2	1.31	1.65	3.58	3.50							
a,b	1.53	2.08	3.78	3.49	1.78	2.27	3.66	3.07	2.19	2.56	3.53

^a For the free chain m_1 is the area spanned by the chain in layer 1 ($L = 7$).

^b The free chain (in a bilayer) is similar to a random chain. The random chain is not subjected to the boundary conditions due to the presence of the interface. For this chain (with $\omega = 0.3$ and $\omega_0 = 1$) $\langle r^2 \rangle^{1/2} = 3.74$ and the number of kinks is 2.58 compared with 2.56 for the free chain (not including kinks between the zeroth and the first bonds).

width of the aggregate, even for free chains. This is consistent with the more general notion that detailed properties such as S_k and $P_n(i)$ are sensitive to the geometry, whereas averaged properties such as (the extremal) $\ln \bar{z}$, \bar{s} , and $\langle \epsilon \rangle$, which are considered below, depend only weakly on the geometry. Other trends, observed from Table I, are quite obvious, e.g., the stretching of the chains (increased $\langle z \rangle$ and $\langle z^2 \rangle$) as L increases, and the different values of $\langle x^2 \rangle$ and $\langle y^2 \rangle$ in cylinders.

Figures 5(A) and 5(B) show, respectively, the conformational entropies and energies of the chains as a function of the core's radius. The entropies attain well defined maxima at different L 's for the different geometries. The location of the maximum increases with the curvature of the hydrophobic core, revealing that, entropically, the optimal micelle radius decreases from spheres to cylinders to bilayers.^{2,12,15} At the minima the entropies are similar to those of the corresponding free chains. The average energy per chain decreases nearly monotonically with L . In bilayers $\langle \epsilon \rangle$ decreases to 0 as $L \rightarrow n(7)$ because when $L = n$ the chain is fully stretched (no kinks). (In this limit $\bar{s} = 0$.) In spheres $\langle \epsilon \rangle$ approaches a finite value since even when $n = L$ ($m_1 \sim 3$) the chains must be partly folded in order to fill the core's volume. In cylinders $\langle \epsilon \rangle$ displays an intermediate behavior, as usual. The slow decrease in $\langle \epsilon \rangle$ as L falls below ~ 4 is expected. When the radius is small the chains are preferentially aligned along the cylinder axis making, on the average, fewer kinks. This, of course, is accompanied by an entropic price, as indicated in Fig. 5(A).

The conformational free energies of the chains in the different geometries are shown in Figs. 6(A) and 6(B) as functions of L and the headgroup area, respectively. Comparison of Fig. 6(A) with Figs. 5(A) and 5(B) reveals that the positions and depths of the minima in $-kT \ln \bar{z} = \langle \epsilon \rangle - T\bar{s}$ are mainly determined by the entropic term. In fact, at the mini-

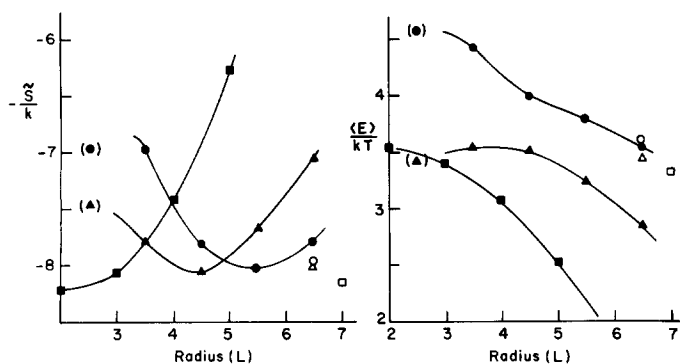


FIG. 5. The conformational entropy (A) and average energy (B) per chain for different aggregate geometries. Squares—planar bilayer, triangles—cylinder, circles—sphere. L is the bilayers' half-thickness. In spheres and cylinders the radius is $L/2$ (See Fig. 1). The open symbols mark the values corresponding to free chains. (Squares for bilayers, etc. For all free chains $L = 7$). All values are for chains packed at liquid density. Note that for planar bilayers with $L = n = 7$ this implies $m_1 = 1$. In this case the chain is fully extended (all-*trans*), i.e., only the fully extended (no kinks) conformation is possible so that $s = 0$ and $\langle \epsilon \rangle = 0$. The points in brackets ($L = 3$ for spheres and cylinders) describe very small and physically irrelevant aggregates and are sensitive to the assumptions of the model (see the text). Similarly, the case of bilayers with $L = 1$ is not shown since it corresponds to a very high head-group area. (The maximum in s is slightly above $L = 2$.)

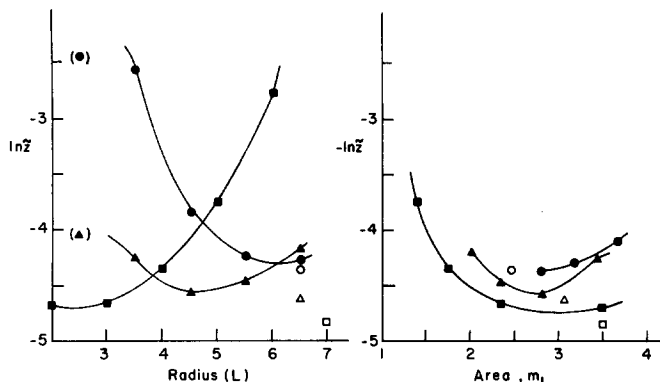


FIG. 6. The conformational free energy per chain (in units of kT) in aggregates of different geometries as a function of the core's radius (A) and the average area per head group (B). Symbols are as in Fig. 5. The minimum in $-\ln \bar{z}$ for bilayers is at $L \gtrsim 2$ and $m_1 \simeq 3$. For cylinders and spheres $m_1 \gtrsim 2$ and 3, respectively, due to geometric packing constraints, see Eq. (11). (Notice that m_1 is the area in layer $i = 1$ of our model, see Fig. 1. The area at the interface is somewhat higher.) Note that whenever two or more aggregate shapes are possible for a given m_1 value, $-\ln \bar{z}$ is the lowest for the least curved structure.

ma in $(-\ln \bar{z})$ the energetic terms corresponding to the three geometries are essentially the same. The differences in $-\ln \bar{z}$ are due primarily to the differences in entropy. Thus, the *packing constraints* which determine the entropy—and not internal energies—are dictating the preferred chain organization.

For a given geometry the minimal value of the conformational free energy is very close to the corresponding value for the free chain. At the L values where the minima are attained $\langle r^2 \rangle$ is about the same for all geometries (see Table I), and is similar to $\langle r^2 \rangle$ of the free and random chains. In other words, as previously suggested by Tanford,⁵ as far as the conformational degrees of freedom only are concerned, the optimal core radius (or, equivalently, the head-group area) is the one which enables the chains to behave as closely as possible to their behavior in the bulk liquid. Note however that in order that $\langle r^2 \rangle$, or other measures of the "liquidity" of the chain (such as $-\ln \bar{z}$), will be similar in different geometries, L must be different.

Figure 6(B) reveals that the minimum in the conformational free energy occurs at about the same average head group for all geometries. Gruen^{15(c)} obtained a very similar result (for a more realistic chain model) except that he finds that all minima obtain for about the same "volume weighted" area per chain, \bar{A} . In terms of Eq. (11) \bar{A} may be defined as $\bar{A} = \sum_i m_i A_i / \sum m_i$. In the "continuous limit", $L \gg 1$, this yields: $\bar{A} = n/L$, $(4n/3L)$, and $(9n/5L)$, for bilayers, cylinders, and spheres, respectively. In the same limit, the corresponding areas per head group, $A \propto m_1$, are $A = n/L$, $2n/L$, and $3n/L$; hence $A/\bar{A} = 1$, $3/2$, and $5/3$, respectively. Since the minima in $-\ln \bar{z}$ are quite shallow (either as a function of A or as a function of \bar{A}) it is not surprising that our findings are similar to those of Ref. 15(c).

The absolute values of the differences between the minimal chain's free energies in the different geometries are small; ~ 0.1 – $0.3 kT$ for our model chains. (Similar results were obtained for alkyl chains.^{12,15}) Recall however, that these values are on the order of the variations in the total

amphiphiles' chemical potential ($\delta\mu$ of transfer from one geometrical environment to another^{1,16,17}). Hence, ignoring such differences in analyzing the relative stabilities of different micellar shapes (such as spheres vs rods) might lead to erroneous conclusions. In a recent paper²¹ we show in particular how these chain free energy effects can alter the size and shape distributions in dilute solution.

As discussed in part I, geometric constraints set limits on the possible values of the head-group areas.^{5,17} For some values of m_1 , two or more micellar geometries are allowed. For example, if $m_1 > 3$ bilayers, cylinders and spheres are all possible. Figure 6(B) shows that for a given m_1 , the geometry with the lowest surface curvature corresponds to the lowest free energy. Head-group interactions will not change this hierarchy as they depend on $m_1(\propto A)$ only (apart from small curvature corrections^{5,17,18}). Smaller aggregates have higher curvatures. Hence the only preference for such aggregates is that they are favored entropically ["translational" and "mixing" entropies, *not* the conformational entropy of Fig. 5(A)]. At very low amphiphile concentrations, close to the cmc, the entropy term is always dominant. But as the concentration is increased and micelles start growing, the conformational contribution, $-kT \ln \bar{z}$, may be important and should be included in analyses of micelle formation and growth.

It should be remembered that the numerical values of \bar{z} , $\langle \epsilon \rangle$, and $\ln \bar{z}$ for our model chains differ from those of real (alkyl) chains. For free (and random) chains approximate scaling laws can be used to translate from one model to another. The geometric constraints in micelles complicate the transformation. Thus, the numerical values quoted above should be regarded only as order of magnitude estimates. At the same time it should be noted that the results presented above for the "cubic" model chains are in good qualitative agreement with detailed calculations for more realistic model chain^{12,15} and with available experimental data.

IV. SUMMARY AND CONCLUSIONS

The numerical results presented in the previous section reveal that the conformational properties of hydrocarbon chains in micelles and bilayers (in their "liquid" state) are governed, primarily, by packing constraints. Internal energy (chain flexibility) effects play a secondary role (except of course, when the chains are very stiff—i.e., at low temperatures or if the kink energies are unusually high). We also found that the extent of chain ordering, along the normal to the micellar interface, decreases from the head group towards the chain end, for all three geometries that have been analyzed. The absolute values of the bond order parameters decrease as the average area per head group increases, and as the micellar radius (bilayer's thickness) decreases. All these findings are consistent with available experimental data¹⁹ or more detailed calculations.¹⁵ The calculations indicate that chain interdigitation (midplane crossing) in bilayers is significant, particularly for large head-group areas.

As mentioned in the previous section, in part I and (in detail) elsewhere²⁰ our pdf of chain conformations [Eq. (1)] is similar to the one (independently) proposed by Gruen.^{12,15} It

is therefore not surprising that our findings for the model chains (Secs. II and III) and "real" chains (part I) are similar to those in Refs. 12 and 15. On the other hand, some of our conclusions differ from those of Dill and Flory³ and of Dill and Cantor,⁴ whose theories are based on the same physical assumptions as ours, but whose $P(a)$'s are different. In particular Dill and Flory found that if the chains are completely flexible (i.e., zero kink energy), the bond order parameters of chains packed in spherical and cylindrical micelles increase towards the chain end. Dill and Cantor, using a somewhat different model, concluded that this behavior is reversed (and thus agrees with experiment), only if the chain is not freely flexible. As noted above this conclusion is at variance with our findings. More detailed comparisons of the various "single chain" theories for chain conformational statistics in micellar aggregates may be found in Ref. 20.

Our results for the geometry dependence of the conformational free energy per chain suggest that this may be a significant contribution to μ^0 , the micelle's standard chemical potential. In the current models of amphiphile self-assembly this contribution is treated as a constant.^{5,17} We intend to examine this assumption by incorporating the conformational contributions into μ^0 and calculating resulting effects on micellar size and shape distributions in aqueous solutions. Calculations for real (rotational-isomeric-state) chains, rather than the model chains considered in this paper, are already in progress. The extension of our theory to mixed aggregates is straightforward and we intend, in particular, to apply our chain conformational analysis to study the molecular and thermodynamic parameters governing the structure and stability of such aggregates.

ACKNOWLEDGMENTS

A.B-S thanks the fund for Basic Research, administered by the Israel Academy of Sciences and Humanities. The Fritz Haber Center is supported by the Minerva Gesellschaft für die Forschung, mbH München, BRD. WMG thanks the National Science Foundation and the ACS Petroleum Research Fund for financial support.

¹A. Ben-Shaul, I. Szleifer, and W. M. Gelbart, *J. Chem. Phys.* **83**, 3597 (1985).

²(a) A. Ben-Shaul, I. Szleifer, and W. M. Gelbart, *Proc. Natl. Acad. Sci. U.S.A.* **81**, 4601 (1984); (b) *Physics of Amphiphiles, Micelles, Vesicles and Microemulsions*, edited by V. Degiorgio and M. Corti (North Holland, Amsterdam, 1985).

³K. A. Dill and P. J. Flory, *Proc. Natl. Acad. Sci. U.S.A.* **77**, 3115 (1980); **78**, 676 (1981).

⁴(a) K. A. Dill and R. S. Cantor, *Macromolecules* **17**, 380 (1984); (b) R. S. Cantor and K. A. Dill, *ibid.* **17**, 384 (1984); (c) K. A. Dill, D. E. Koppel, R. S. Cantor, J. D. Dill, D. Bendedouch, and S.-H. Chen, *Nature* **309**, 42 (1984).

⁵C. Tanford, *The Hydrophobic Effect*, 2nd ed. (Wiley, New York, 1980).

⁶P. J. Flory, *Statistical Mechanics of Chain Molecules* (Wiley, New York, 1969).

⁷In our model calculations the zeroth bond is assumed to be normal to the core's interface. The uncertainty associated with this approximation is incorporated, partly and implicitly, in ω_0 which is treated as a parameter. Different values for ω and ω_0 were also used by Dill and Cantor (Ref. 4). Gruen (Refs. 12 and 15) who studied real chains in various geometries used

- a sampling procedure for averaging over head-group positions and zeroth bond orientations. A similar procedure has been used by us for obtaining the results shown in Fig. 4 of part I (Ref. 1).
- ⁸(a) S. W. Haan and L. R. Pratt, *Chem. Phys. Lett.* **79**, 436 (1981); (b) B. Owenson and L. R. Pratt, *J. Phys. Chem.* **88**, 2905 (1984).
- ⁹M. A. Winnik, D. Rigby, R. F. T. Stepto, and B. Lemaire, *Macromolecules* **13**, 699 (1980). The authors use 0.6 kcal/mol for the *gauche* energy and 1.9 kcal/mol for the pentane conformation (see Ref. 6). We have used their calculated results for $\langle r^2 \rangle$, for chains with CCC bond angle of 112° .
- ¹⁰(a) D. Bendedouch, S.-H. Chen, and W. C. Kohler, *J. Phys. Chem.* **87**, 153 (1983); (b) B. Cabane, R. Duplessix, and T. Zemb, in *Surfactants in Solution*, edited by K. L. Mittal and B. Lindman (Plenum, New York, 1984).
- ¹¹The average area per head group, A , is usually "measured" at the hydrocarbon-water interface. For the curved geometries this implies that A is slightly larger than our m_1 , see Fig. 1.
- ¹²D. W. R. Gruen and E. H. B. deLacey, in *Surfactants in Solution*, edited by K. L. Mittal and B. Lindman (Plenum, New York, 1984), Vol. 1, p. 279.
- ¹³Like ordinary chains in micelles, a "free chain" is anchored to the core's interface and confined to its inner side. However, this (hypothetical) chain has no neighbors so that $\pi_i = 0$, cf. Eq. (1) (see also Ref. 1).
- ¹⁴See, e.g., J. Seelig and A. Seelig, *Q. Rev. Biophys.* **13**, 19 (1980).
- ¹⁵(a) D. W. R. Gruen, in *Surfactants in Solution*, edited by K. L. Mittal and P. Bothorel (Plenum, New York, 1985); (b) *J. Phys. Chem.* **89**, 146 (1985); (c) *Science* (in press).
- ¹⁶P. J. Missel, N. A. Mazer, C. B. Benedek, C. Y. Young, and M. C. Carey, *J. Phys. Chem.* **84**, 1044 (1980).
- ¹⁷(a) J. N. Israelachvili, D. J. Mitchell, and B. W. Ninham, *J. Chem. Soc. Faraday Trans. 2*, **72**, 1525 (1976); (b) J. N. Israelachvili, S. Marcelja, and R. G. Horn, *Q. Rev. Biophys.* **13**, 121 (1980).
- ¹⁸D. J. Mitchell and B. W. Ninham, *J. Chem. Soc. Faraday Trans. 2* **77**, 601 (1981).
- ¹⁹(a) See, e.g., J. Charvolin, *J. Chim. Phys.* **80**, 15 (1983); (b) J. Charvolin and Y. Hendrikx, in *NMR in Liquid-Crystals*, edited by J. W. Emsley and G. Luckhurst (Reidel, Dordrecht, 1985); (c) T. Ahlén, O. Söderman, H. Walderhaug, and B. Lindman, in *Surfactants in Solution*, edited by K. L. Mittal and B. Lindman (Plenum, New York, 1984), Vol. 1, p. 107; (d) see also, Refs. 1, 14, and 15 and references cited therein.
- ²⁰I. Szeleifer, A. Ben-Shaul, and W. M. Gelbart, in *Surfactants in Solution*, edited by K. L. Mittal and P. Bothorel (Plenum, New York, to be published).
- ²¹W. E. McMullen, A. Ben-Shaul, and W. M. Gelbart, *J. Colloid Interface Sci.* **98**, 523 (1984).